PRAMANA
— journal of
physics

Vol. 75, No. 3
September 2010
pp. 513–522

Electron irradiation effects on 4-amino-5-mercapto-3-[1-(4-isobutylphenyl)ethyl]-1,2,4-triazole single crystal

VIJAYALAKSHMI RAO and K NASEEMA*
Department of Materials Science, Mangalore University, Mangalagangothri 574 199, Mangalore, India
*Corresponding author. E-mail: vijrao@yahoo.com; vijraobrns@rediffmail.com

MS received 5 January 2010; revised 12 February 2010; accepted 17 March 2010

Abstract. In this paper, we report the electron irradiation effects on the properties of an organic NLO single crystal of 4-amino-5-mercapto-3-[1-(4-isobutylphenyl)ethyl]-1,2,4-triazole. The crystal was irradiated with electron beam of different doses and was characterized by powder XRD, UV–Vis, FTIR, DSC, microhardness and SHG measurements. In XRD, the peaks are shifted due to irradiation. The SHG efficiency has been found to enhance rapidly with irradiation. The investigation of the influence of electron irradiation on the surface morphology of the grown crystal reveals the formation of craters on the surface. The laser damage threshold remains constant as the dose rate increases whereas refractive index increases after irradiation.

Keywords. Electron irradiation; non-linear optical crystal; organic material.

PACS Nos 42.70.Mp; 42.65.k; 42.65.ky; 42.79.Nv

1. Introduction

Nonlinear optics is the study of interaction of radiation with matter in which certain variables describing the response of matter (such as electric polarization or power absorption) are not proportional to the variables describing the radiation (such as electric field strength or energy flux). Nonlinear optical materials play a major role in the technology of photonics. In all materials, nonlinear effects of various types are observed at sufficiently high light intensities. Frequency doubling is one of the visually dramatic features among the nonlinear optical processes [1].

High-energy electron irradiation produces electronic excitation/ionization in solids, which leads to many changes in their physical properties. It is known that when an electron beam passes through matter, it causes damage, which depends on the energy and flux density of the incident electron beam [2–6]. It is generally pictured that atomic displacements are primarily induced by elastic collisions and not by electronic excitation or ionization. However, slowing down the energetic

electrons in insulator targets is known to induce structural changes called lateral tracks, resulting from the atomic displacements in the material along the path of the electron [7,8]. Electronic and nuclear energy depositions reach up to a few keV/A where structural changes can be expected.

Disordering the crystal lattice and their composition by electron irradiation produces changes in electrical conductivity and optical properties depending upon the extent of damage caused. SHG was observed in the electron beam irradiated GeS_2–In_2S_3–CaS chalcogenide glasses. The SHG has increased with the increasing irradiated current [9]. Introduction of stress is a powerful means to enhance nonlinear optical susceptibility. $BaTiO_3$ was stress-induced by laser molecular beam epitaxy and it was found that SHG is enhanced [10]. These considerations motivated us to study the effect of high-energy electron irradiation on the crystal and to characterize by different techniques.

The 1,2,4-triazole derivatives show antibacterial, antifungal, antitubercular, anticancer, antitumor, anticonvulsant, anti-inflammatory and analgesic properties. Quantitative measurements of the second harmonic generation of powdered 4-amino-1,2,4-triazol-1-ium hydrogen oxalate confirms its NLO property [11]. Since very little studies have been carried out in this class of compound, to explore its nonlinear optical properties, we have synthesized the title compound 4-amino-5-mercapto-3-[1-(4-isobutylphenyl)ethyl]-1,2,4-triazole (AMIT), grown the single crystals and reported some of its characterizations [12]. Here we report the characterization of the irradiated crystal using powder XRD, UV–Vis, FTIR, DSC, microhardness and SHG measurements. The irradiation effect on refractive index and laser damage threshold are also reported.

2. Experimental

2.1 *Material synthesis and crystal growth*

The title compound was synthesized and the single crystals were grown by slow evaporation [12]. It belongs to the monoclinic system with the space group $P2_1$. The lattice parameters are $a = 5.9720$ Å, $b = 8.5153$ Å, $c = 14.8271$ Å, $\beta = 97.223°$, $V = 748.03$ Å^3, $Z = 2$ and density $D = 1.227$ mg m^{-3}.

2.2 *Electron irradiation*

Specifications of electron beam used for irradiation are as follows: beam energy: 8 MeV, beam current: 25–30 mA, beam size: 5 mm × 5 mm, pulse repetition rate: 50 Hz, pulse width: 2.5 μs, dose rate: 1 kGy/min (Fricke dosimetry). The sample was kept at a distance of 30 cm from the target. The single crystals of AMIT were irradiated at room temperature with a dose of 0.5, 1 and 1.5 kGy.

3. Characterization

3.1 *XRD studies*

The XRD pattern of the powdered crystal was recorded in a BRUKER AXS-D 8 Advance with copper target ($\lambda = 1.54$ Å). The revelation of well-defined Brag reflections at specific 2θ angles in the diffraction pattern suggest crystallinity of the sample. Due to irradiation, the peaks were shifted (figures 1a–c). All the samples show peak around 6°. This peak for pristine sample corresponds to a count of 474, whereas it decreases to 92 and 60, for 0.5 kGy absorbance and 1.5 kGy absorbance respectively. Here we can see a decrease in intensity of peaks as absorbed dose increases. For the pristine sample, the next peak is seen around 21°. Corresponding to this angle, the peak intensity of the irradiated samples are very low. Around 27°, peaks of different intensities are seen for the pristine and 1.5 kGy irradiated samples, while its presence is almost negligible at 0.5 kGy. But a very strong peak around 42° is observed in the XRD of the 0.5 kGy irradiated sample, which is not seen in the pristine and 1.5 kGy irradiated samples. This clearly indicates that the electron–solid interaction is capable of producing electronic excitations leading to thermal spikes that produce defects along the path of electrons.

3.2 *UV–Vis spectral analysis*

UV–visible spectrum of the grown crystal was recorded using a SHIMADZU UV–VIS–NIR scanning spectrophotometer, model 3101 PC. The solution grown organic crystal, AMIT, did not show any colour change due to irradiation. The dose dependences of the optical absorption spectra of all these irradiated samples were recorded. The UV–visible spectra of the irradiated single crystals did not show any change when compared with unirradiated crystal.

3.3 *FTIR spectral analysis*

The FTIR spectra of the pristine and irradiated crystals were recorded in the KBr phase within the frequency region of 400–4000 cm^{-1}, using SHIMADZU 8400S FTIR spectrometer. FTIR spectra of the pristine and irradiated crystals were compared with each other. No significant changes are observed in the spectra. The absence of a prominent new peak shows that there is no significant formation of intermediate chemically distinct material during irradiation.

3.4 *Thermal analysis (DSC)*

The DSC analysis was done between 30 and 200°C at a heating rate of 10°C/min in the nitrogen atmosphere. From the peak, it is inferred that the melting takes place at 168°C, which is the same as that of the pristine sample.

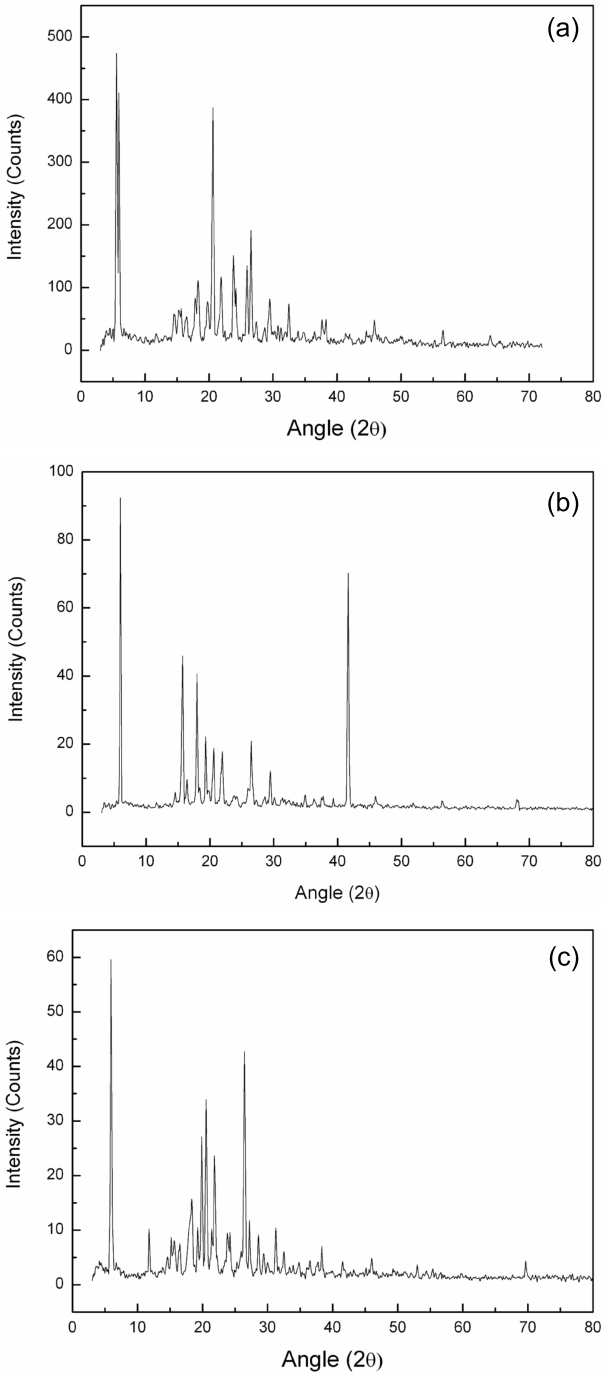

Figure 1. 1-Powder XRD patterns of (**a**) pristine, (**b**) 0.5 kGy-irradiated and (**c**) 1.5 kGy-irradiated samples of AMIT. The peaks are shifted due to irradiation.

Electron irradiation effects

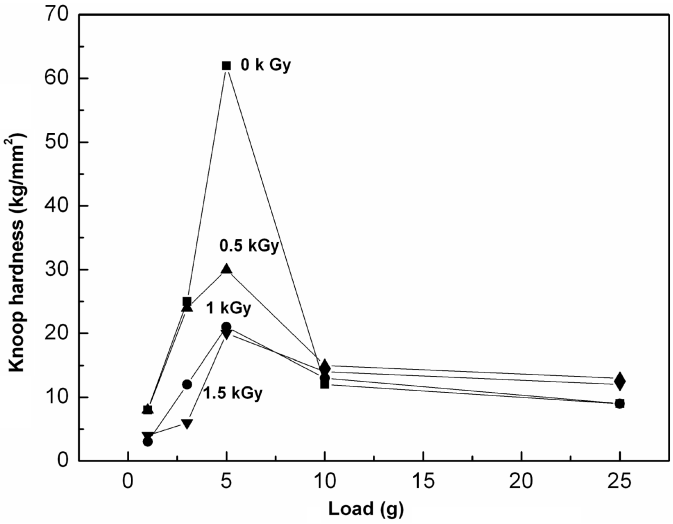

Figure 2. Load vs. hardness of AMIT for various electron fluences. Hardness number decreases corresponding to the single peak for a load of 5 g.

3.5 *Microhardnes measurement*

Knoop hardness studies on pristine and electron-irradiated crystals were carried out using CLEMEX digital microhardness tester. A decrease in the hardness corresponding to the single peak for a load of 5 g is observed as the irradiation dose increases (figure 2). This shows that the dislocations taking place are different in crystals irradiated with different doses and substantiates the formation of isolated defect centres and weak lattice stresses on the surface.

3.6 *SHG measurement*

The study of NLO conversion efficiency has been carried out using modified experimental set-up of Kurtz & Perry. A Q-switched Nd:YAG laser beam of wavelength 1064 nm, with an input power of 2.2 mJ and a pulse width of 8 ns with a repetition rate of 10 Hz was used. The pristine and irradiated crystals were powdered and packed in microcapillaries of uniform bore and exposed to laser radiation. The output from the sample was monochromated to collect the intensity of 532 nm component. The output was measured using a photomultiplier tube (PMT) and displayed on a storage oscilloscope. The SH signals of the crystal samples relative to KDP were reliably measured, by fixing the fundamental laser energy constant. The intensity of the second harmonic generation effect of the pristine sample is 30% that of KDP and the effect is phase matchable. A solution-grown KDP crystal, pulverized to have the particle size the same as that of the samples, was used as the reference material in the present measurement. The SHG conversion efficiency of the irradiated sample was found to be increasing with increasing dose rate

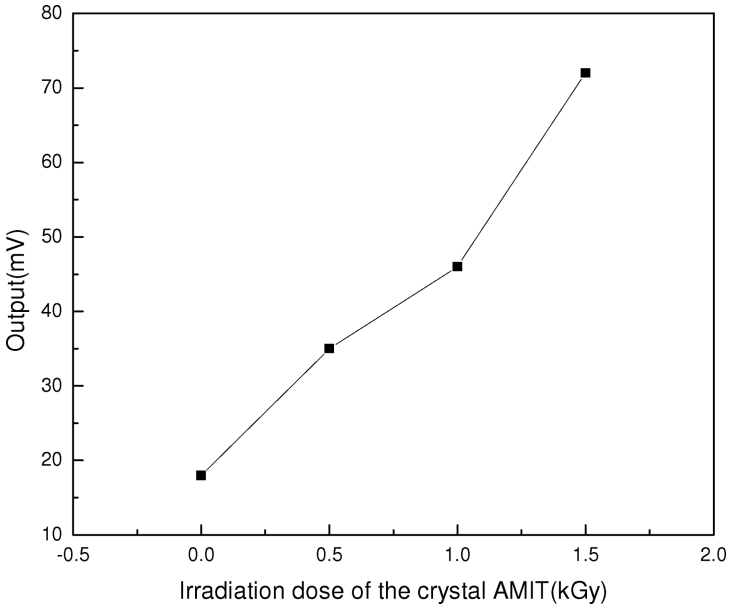

Figure 3. SHG response of pristine and irradiated AMIT. SHG increases with absorbed dose.

(figure 3). The increase in the SHG output at higher fluence implies that higher concentration of free radicals favours the movement of unpaired electrons along the radical sites, which increases the second-order polarizability of the molecular crystal. CH and NH_2 radicals produced after irradiation were trapped in the crystal lattice, and the concentration of free electron radicals is proportional to the radiation dose absorbed by the sample [13,14]. A similar observation has been reported for L-alanine and L-threonine single crystals [10,15–17]. Introduction of stress by electron beam irradiation enhances nonlinear optical susceptibility. Reaching second-order effects requires favourable alignment of the molecule within the crystal structure [18] and it appears that it is well facilitated by irradiation.

3.7 *SEM*

The SEM provides information about the topographical features, morphology, phase distribution, compositional differences, crystal orientation etc. The influence of electron irradiation on the surface morphology of the grown crystal reveals the formation of craters of 10 μm average size with an electron beam of size 5 mm $\times$ 5 mm, when compared to the pristine sample (figures 4a and 4b). This can be attributed to the shock waves generated in the crystal due to electron irradiation. Many research groups have explained the formation of craters in solids using the shock waves present in solids due to bombardment [19]. This type of craters have been imaged by AFM on the surface of L-valine single crystals after bombardment with MeV ions [20–24] and also on the organic benzoyl glycine crystals [25] and

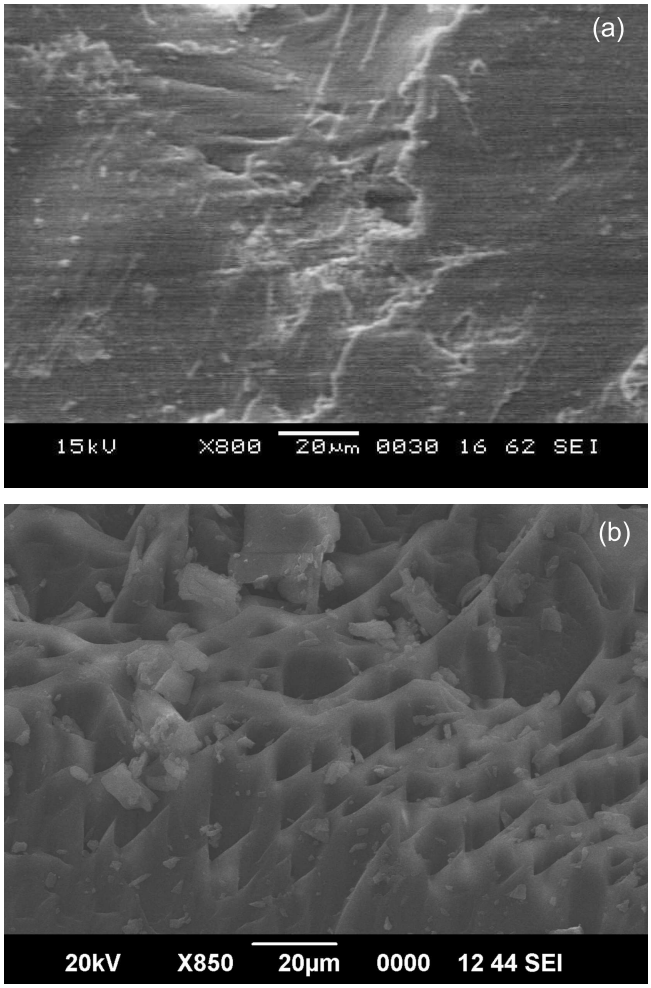

Figure 4. SEM micrographs of (**a**) pristine and (**b**) electron-irradiated AMIT. Craters are formed on the surface due to irradiation.

acetoacetanilide [26]. Methyl parahydroxy benzoate crystals bombarded with zinc ions exhibit craters of 50 nm mean diameter [27]. Craters are produced at high energy losses. The binding energy of the molecules is a few eV, while the energy received by each molecule is about a few MeV. Hence molecules may have been fragmented or ejected [28]. Most of the molecules ejected from the surface region would have been fragmented as the energy density close to the track is very high.

3.8 *Laser damage threshold*

One of the most important considerations in the choice of a material for nonlinear optical applications is its optical damage tolerance. The laser damage threshold

studies have been performed on the pristine and the irradiated crystals. As we go on increasing the dose rate, no change was found for the laser damage threshold of the irradiated crystals which was found to remain constant at 1.89 GW/cm^2.

3.9 *Refractive index*

Brewster's angle method calls for extremely precise intensity measurements as a function of crystal angle. Using a red (He–Ne) laser of 633 nm wavelength, the refractive indices of the crystal before and after electron irradiation are measured by this technique. Though the refractive index, n, of the pristine sample is 1.47, due to electron irradiation, the refractive index is found to be increased to 1.51. The increase in refractive index after irradiation proves the ability of fabricating planar waveguides by electron irradiation in this type of materials and increasing their applicability in various nonlinear applications. Ion implantation has been applied to modulate refractive index and to fabricate optical waveguides in insulating materials [29,30]. In the case of inorganic NLO crystals like KTP and LBO, a decrease in refractive index due to He ion irradiation has been reported [31,32]. The refractive index is found to decrease in barium strontium borate crystals due to both ion and electron irradiations [33]. It is reported that fabrication of embedded waveguides in lithium niobate crystals is possible by radiation damage [34].

Waveguiding has been demonstrated in DAST channel waveguides using 30 keV e-beam irradiation. The refractive index profile in DAST has been measured as a function of the electron range and the electron fluence in DAST (4-N,N-dimethylamino-4′-N′-methyl-stilbazolium tosylate). A reduction of the refractive index has been obtained using an electron fluence of 2.6 mC/cm^2 [35]. Electron beam direct structuring has already been used to create channel waveguides in silica, in which the refractive index was increased in the exposed area [36,37].

It is known that the optical properties of polymers and crystals can be engineered using ion irradiation/implantation [38]. The refractive index of a layer at a certain depth from the surface can be changed by creating damages using irradiation. Such a layer, whose refractive index is different from its surroundings, acts as an optical waveguide. Since these organic crystals exhibit SHG for lasers, the efficiency of conversion can be enhanced in the channel guide. For this purpose, it is necessary to measure refractive index as a function of depth.

The increase in refractive index may be due to the increased density induced by disordering of the crystal lattice by the ion beam or due to structural defects [39]. In general, in the surface region, the change in refractive index may be positive or negative due to the combination of damage, ionization diffusion effects and electronic polarization change.

4. Conclusion

Single crystals of 4-amino-5-mercapto-3-[1-(4-isobutylphenyl)ethyl]-1,2,4-triazole were grown from ethanol by slow evaporation of the solvent at room temperature. They were irradiated with electron beam of different doses. The pristine and the

irradiated crystals were characterized by different methods. Changes were observed in XRD and microhardness. The SHG efficiency has been found to be increasing four times with irradiation dose, which suggests that electron irradiation can be used to enhance the NLO property of crystals. The investigation of the influence of electron irradiation on the surface morphology of the grown crystal reveals the formation of craters on the surface. The laser damage threshold remains constant as the dose rate increases. The increase in refractive index after irradiation shows the possibility of fabricating planar waveguides by electron irradiation in this type of materials.

Acknowledgement

Authors thank Microtron Centre, Mangalore University for electron irradiation, Dr P K Das, ICPC, IISc, Bangalore for SHG measurement and Dr Narayana Rao, University of Hyderabad, for laser damage threshold measurement.

References

[1] P N Prasad and D J Williams, *Introduction to nonlinear optical effects in organic molecules and polymers* (Wiley, New York, 1991)
[2] N Betz *et al*, *J. Polym. Sci. Polym. Phys.* **B32**, 1493 (1994)
[3] T Stecken Reiter, E Balanzat, H Fuess and C Trautmann, *Nucl. Instrum. Methods* **B131**, 159 (1997)
[4] M Toulemonde, S Bauffard and F Studer, *Nucl. Instrum. Methods* **B91**, 108 (1994)
[5] P D Townsend, *MAPS Vacuum* **44**, 267 (1993)
[6] M Nakanishi, O Sugihara and N Okamoto, *J. Appl. Phys.* **86**, 2393 (1999)
[7] G K Mehta, *Phys. Education* **11**, 245 (1994)
[8] G Ramesh Kumar *et al*, *Radiat. Eff. Defects in Solids* **163**, 223 (2008)
[9] Qiming Liu, Chang Gau, Hong Li and Xiujian Zhao, *Solid State Commun.* **149**, 266 (2009)
[10] Tong Zhao, Hinbin Lu, Fan Chen, Guozhen Yang and Zhenghao Chen, *J. Appl. Phys.* **87**, 7448 (2000)
[11] Irena Matulkova, Ivan Němec, Karel Teubner, Petr Němec and Zdenek Micka, *J. Mol. Struc.* **873**, 46 (2008)
[12] K Naseema, Vijayalakshmi Rao, K V Sujith and Balakrishna Kalluraya, *Pramana – J. Phys.* **73**, 719 (2009)
[13] E Winkler, P Etchegoin, A Fainstein and C Fainstein, *Phys. Rev.* **B57**, 13477 (1998)
[14] G Ramesh Kumar, S Gokul Raj, K A Bogle, S D Dhole, V N Bhoraskar and R Mohan, *Appl. Surf. Sci.* **254**, 5231 (2008), DOI: 10.1016/j.apsusc.2008.02.030
[15] S Ebraheem, W B Beshir, S Eid, R Sobhy and A Kovacs, *Radiat. Phys. Chem.* **67**, 569 (2003)
[16] R Mishra, S P Tripathy, K K Dwivedi, D T Khathing, S Ghosh, M Muller and D Fink, *Radiat. Meas.* **37**, 247 (2003)
[17] R Vijayalakshmi Rao, P Mohan Rao and M H Shridhar, *Nucl. Instrum. Methods Phys. Res.* **B187**, 331 (2002)
[18] S R Hall, P V Kolinsky, R Jones and S J Allen, *J. Crystal Growth* **79**, 745 (1986)

[19] J Kopniczky, A Hallen and N Keskitalo, *Radiat. Meas.* **25**, 47 (1995)
D D N Baralo Daya, A Hallen and J Erikson, *Nucl. Instrum. Methods* **B106**, 38 (1995)
[20] A P Quist, J Ahlbom, C T Reimann and B U R Sundqvist, *Nucl. Instrum. Methods* **B130**, 164 (1994)
[21] J Eriksson, J Kopniczdy, G Brinkmalm, R M Papaleo, P Demirev, C T Reimann, P Hakansson and B U R Sunqvist *Nucl. Instrum. Methods* **B101**, 142 (1995)
[22] J Kopnizky, A Hallen, N Keskitalo, C T Reimann and B U R Sundqvist, *Radiat. Meas.* **25**, 47 (1995)
[23] D D N Barlodaya, A Hallen, J Eriksson, J Kopniczky and R Papaleo, *Nucl. Instrum. Methods* **B106**, 38 (1995)
[24] T Reimann, P Hakansson, B U R Sundqvist, A Brunelle, S Dellanegra and Y Le Beyec, *Nucl. Instrum. Methods* **B106**, 38 (1995)
[25] J Eriksson, J Kopniczky, P Demirev, R M Papaleo, G Brinkmalam, C T Reimann, P Hakansson and B U R Sundqvist, *Nucl. Instrum. Methods* **B107**, 281 (1996)
[26] H S Nagaraja, Fohnesorge, D K Avasthi, R Neumann and P Mohan Rao, *Appl. Phys.* **A71**, 337 (2000)
[27] H S Nagaraja, *Radiation effects on laboratory grown organic single crystals*, Ph.D. Thesis (Mangalore University, 2001)
[28] C T Reimann, *Nucl. Instrum. Methods* **B95**, 181 (1995)
[29] P D Townsend, *Rep. Prog. Phys.* **50**, 501 (1987)
[30] P D Townsend, *Cryst. Lattice Defects* **18**, 377 (1989)
[31] E L Babsil and P D Townsend, *Appl. Phys. Lett.* **59**, 384 (1991)
[32] D Flock and P Gunter, *Opt. Commun.* **90**, 304 (1992)
[33] S Ishwar Bhat and P Mohan Rao, *Surface coatings and technology* **158**, 725 (2002)
[34] K Peithmann, M R Zamani-meymian, M Haaks, K Maier, B Andreas, K Buse and H Modrow, *Appl. Phys.* **B82**, 419 (2006)
[35] Lukas Mutter, Manuel Koechlin, Mojca Jazbin Sek and Peter Gunter, *Optics Express* **15**, 16828 (2007)
[36] A J Houghton and P D Townsend, *Appl. Phys. Lett.* **29**, 565 (1976)
[37] S G Blanco, A Glidle, J H Davies, J S Aitchison and J M Cooper, *Appl. Phys. Lett.* **79**, 2889 (2001)
[38] S Brunner, D Ruck, W Frank, F Linke, A Schosser and U Behringer, *Nucl. Instrum. Methods* **B89**, 373 (1994)
[39] P Sreeramana Aithal, *Growth and characterization of some optoelectronic and nonlinear optical single crystals*, Ph.D. Thesis (Mangalore University, 1996)